Weighted Random Forest using Gaze Distributions Measured from Observers for Gender Classification

Sayaka Yamaguchi[1], Masashi Nishiyama[2] and Yoshio Iwai[2]

[1]*Graduate School of Sustainability Science, Tottori University, Tottori, Japan*
[2]*Graduate School of Engineering, Tottori University, Tottori, Japan*

Keywords: Gender Classification, Random Forest, Gaze Distribution.

Abstract: We propose a method to improve gender classification from pedestrian images using a random forest weighted by a gaze distribution. When training samples contain a bias in the background surrounding pedestrians, a random forest classifier may incorrectly include the background attributes as discriminative features, thereby degrading the performance of gender classification on test samples. To solve the problem, we use a gaze distribution map measured from observers completing a gender classification task for pedestrian images. Our method uses the gaze distribution to assign weights when generating a random forest. Each decision tree of the random forest then extracts discriminative features from the regions corresponding to the predominant gaze locations. We investigated the effectiveness of our weighted random forest using a gaze distribution by comparing the following alternatives: assigning weights for feature selection, assigning weights for feature values, and assigning weights for information gains. We compare the gender classification results of our method with those of existing random forest methods. Experimental results show our random forest using information gains weighted according to the gaze distribution significantly improved the accuracy of gender classification on a publicly available dataset.

1 INTRODUCTION

Gender classification using pedestrian images is an integral part of developing a novel marketing system in a general merchandise store. Existing methods (Antipov et al., 2015; Schumann and Stiefelhagen, 2017) have improved the accuracy of gender classification using deep learning or other machine learning techniques. The existing methods require a large number of training samples to attain high-accuracy classification results. Collecting a large number of training samples entails a high cost. Furthermore, the training samples may include an unexpected bias. For instance, the background surrounding the pedestrians in the training samples forms a bias if the pedestrian images are collected in a specific place. This bias may cause the gender classifier to incorrectly regard the background as discriminative features.

To avoid the problems caused by the bias from the background surrounding the pedestrians in the training samples, we must extract discriminative features from pedestrian images for gender classification. A human can correctly distinguish the gender of a pedestrian in an image by examining body characteristics and excluding the background. We use this human visual capability to aid in feature extraction for gender classification, to address the scenario whereby the background in the training samples contains a bias. Recent studies have proposed extracting discriminative features by incorporating a gaze distribution measured from observers viewing stimulus images (Sattar et al., 2017; Murrugarra-Llerena and Kovashka, 2017; Nishiyama et al., 2018). Although these existing methods do not mention the background bias in the training samples, the method is applicable to the problems caused by the bias. In particular, Nishiyama et al. explores the use of the gaze distribution to design a preprocessing technique for a gender classifier. A gaze distribution was measured from observers while determining the gender of pedestrians in images. This method extracted features by assigning large weights for body regions corresponding to the gaze locations measured from the observers. However, this method did not consider including the gaze distribution to generate the classifier. Rather, this method simply used the gaze distribution to assign weights to the pixel values in the pedestrian images as a preprocessing step for classification.

Here, we consider using the gaze distribution when generating a random forest (Breiman, 2001). As shown in (Rokach, 2016), a random forest consisting of many decision trees can obtain a high classification performance for various applications. The process of generating the decision trees is based on randomness according to the uniform distribution. In this paper, we consider tuning the randomness according to the gaze distribution instead of the uniform distribution. To do this, we use a weighted random forest (Amaratunga et al., 2008; Winham et al., 2013; Maudes et al., 2012). Amaratunga et al. assigned large weights to the training samples contributing most to the classification performance. Winham et al. assigned large weights to the votes in the decision trees that contributed most to the classification performance. However, these existing methods are not easily altered to include a gaze distribution because the methods did not consider the positions of features in the pedestrian images. Maudes et al. assigned random weights to features and information gains when generating the decision trees to increase noise tolerance. The features and information gains are deeply relevant to positions in pedestrian images. However, the existing method simply used random weights and did not consider a gaze distribution.

To this end, we hypothesize that the features and information gains of the random forest depend on a gaze distribution that considers the frequent gaze locations of observers. We propose a method to correctly classify gender by generating a weighted random forest using a gaze distribution on training samples that contain a background bias. To design this novel method of generating a random forest, we investigated the following alternatives: assigning weights for feature selection, assigning weights for feature values, and assigning weights for the information gains. We evaluated the accuracy of the gender classification using these alternatives on a publicly available dataset. We confirmed that our method of assigning to the information gains outperformed the other methods.

2 BACKGROUND BIAS IN TRAINING SAMPLES

Training samples collected for gender classification may contain specific objects in the background surrounding the pedestrians, thereby introducing a bias. Here, we discuss a case whereby the training samples showing males contain a fence in the background while the training samples showing females do not, as shown in Figure 1. This case may be prevalent
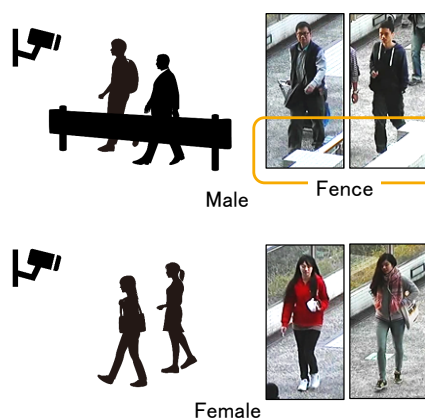

Figure 1: Examples of training samples containing a bias from the background surrounding the pedestrians.

when many females appear in the vicinity of a certain camera (e.g., near a cosmetics counter), and many males appear in the vicinity of another camera (e.g., around a menswear section). In our preliminary experiments, we observed that the accuracy of gender classification declined when using training samples containing a background bias (e.g., the presence or absence of a fence). A random forest gender classifier included the background bias as discriminative features rather than the true differences between the physical appearances. For example, a test sample of a female with a fence in front was incorrectly classified as male. Avoiding this problem generally requires a large number of training samples containing various backgrounds for both genders. When the background is obviously biased, we could modify the pedestrian image collection strategy. In some cases, once the sample collection is already complete, an unexpected bias may be found in the training samples according to the outputs of a gender classifier. Because the collection of training samples is very time-consuming, we may need to use the collected training samples despite their bias. Therefore, our method aims to correctly classify gender using a weighted random forest incorporating a gaze distribution when the training samples contain a background bias.

3 WEIGHTED RANDOM FOREST USING A GAZE DISTRIBUTION

3.1 Overview of Decision Tree Generation

The existing method for generating a random forest (Breiman, 2001) is as follows. Subsets of trai-

ning samples are prepared using bootstrap sampling, and each subset is used to generate a decision tree in the random forest. We denote a pixel of color c_i in the position (x_i, y_i) of a pedestrian image as a feature value $f_i(x_i, y_i, c_i)$. In the field of computer vision (Gall et al., 2011), the difference between pixel values in an image observed from two positions is widely used as a feature value. In this paper, we directly use the pixel values as features to simplify the generation of the decision trees in the random forest.

When generating each decision tree from each subset of training samples, a feature value $f_i(x_i, y_i, c_i)$ and a threshold t_j are randomly selected. The information gain is computed using the selected feature value and selected threshold. The random selection of $f_i(x_i, y_i, c_i)$ and t_j is repeated until M feature values and N thresholds are stored. The stored feature values and thresholds are used to determine a branch condition, where a training sample in a parent node is branched to either the left or right child node. The existing method searches a branch condition using the information gains computed from the candidate parameters $\{x_i, y_i, c_i, t_j\}$. An information gain $I_{i,j}(x_i, y_i, c_i, t_j)$ of a candidate parameter is represented as:

$$I_{i,j}(x_i, y_i, c_i, t_j) = H(S) - \sum_{k \in \{L,R\}} \frac{|S^k|}{|S|} H(S^k), \quad (1)$$

where S is a set of training samples in a parent node, S^k is a set of training samples in a child node, and $H(\ )$ is the entropy. Note that $S^L \cap S^R = \phi$ and $S^L \cup S^R = S$. The branch condition at each node is represented as:

$$\begin{cases} s \in S^L & f(x_i, y_i, c_i) \geq t_j, \\ s \in S^R & \text{otherwise.} \end{cases}$$

Entropy is computed as follows:

$$H(S) = - \sum_{a \in \{male, female\}} p(a) log(p(a)), \quad (2)$$

where $p(a)$ is the ratio of the training samples of gender type a contained in the set S. The candidate parameter set corresponding to the maximum information gain is used as a branch condition from the parent node to the child nodes. The branch condition search is repeated until the depth reaches a preset value.

3.2 Gaze Map

We represent the gaze distribution using the gaze map described in (Nishiyama et al., 2018). To generate a gaze map, observers complete a pedestrian gender classification task on stimulus images, and the observer gaze locations are recorded. The average of the measured gaze locations is computed across different observers and stimulus images. $g(x_i, y_i)$ denotes a
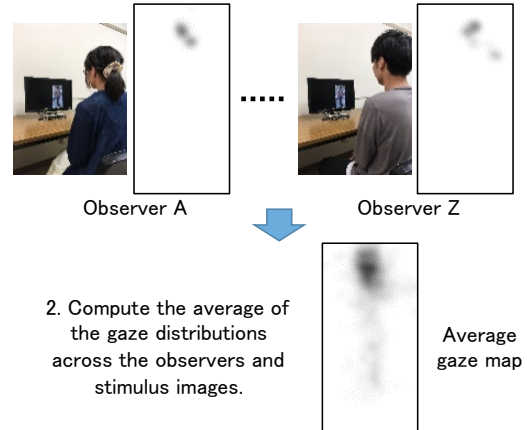

Figure 2: Generating a gaze map from a gender classification task assigned to oberservers.

pixel value at a position (x_i, y_i) of the gaze map. The range of $g(x_i, y_i)$ is set to $[0, 1]$, and the size of the gaze map is equal to that of the stimulus images. Figure 2 shows an overview of the process of generating a gaze map from a gender classification task assigned to multiple observers. In the figure, the dark region in the gaze map represents the most frequent gaze locations gathered from the observers. Nishiyama et al. demonstrated that the head region was the most prevalent gaze location when judging gender from pedestrian images.

3.3 Assigning Weights for Feature Selection

We describe the method of assigning weights for feature selection when generating a random forest. We begin by outlining the existing methods (Breiman, 2001; Maudes et al., 2012). When applying the existing methods for gender classification, the position (x_i, y_i) of a feature value is randomly selected according to the uniform distribution. In contrast, our method selects the position (x_i, y_i) of a feature value according to the gaze distribution where a large weight indicates the areas where the gaze locations of the observers are gathered. Figure 3 shows an overview of our method. The figure demonstrates that the feature values in the dark regions of $g(x_i, y_i)$ (where the gaze locations of observers are gathered) are frequently selected.
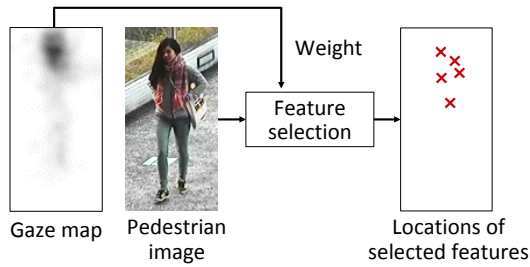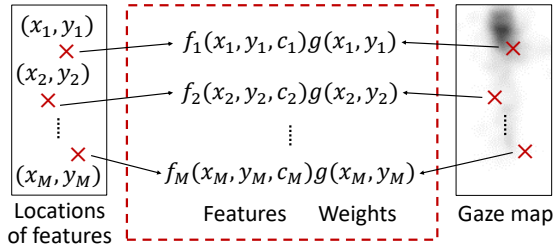
Figure 3: Assigning weights for feature selection.

Figure 4: Assigning weights for feature values.

3.4 Assigning Weights for Feature Values

We describe a method for assigning weights for feature values when generating the random forest. The existing methods (Breiman, 2001; Maudes et al., 2012) did not modify the feature values. Maudes et al. assigned random weights to the feature values according to the uniform distribution. In contrast, our method assigns weights according to the gaze distribution represented as a gaze map $g(x_i, y_i)$ using the following equation:

$$f'(x_i, y_i, c_i) = f(x_i, y_i, c_i)g(x_i, y_i). \qquad (3)$$

Figure 4 shows an overview of our method. In the figure, a weighted feature at position (x_i, y_i) attains a large weight when it corresponds to the dark region of $g(x_i, y_i)$ where the gaze locations of the observers are gathered. Note that the above procedure achieves the same effectiveness as the preprocessing technique described in (Nishiyama et al., 2018).

3.5 Assigning Weights for Information Gains

We describe a method to assign weights for the information gains when generating a random forest. We explain our method by contrasting with the existing methods (Breiman, 2001; Maudes et al., 2012). Breiman computed an information gain from parameter candidates $\{x_i, y_i, c_i, t_j\}$ as described in Section 3.1. Maudes et al. computed information gains using the same approach as Breiman and additionally weighted
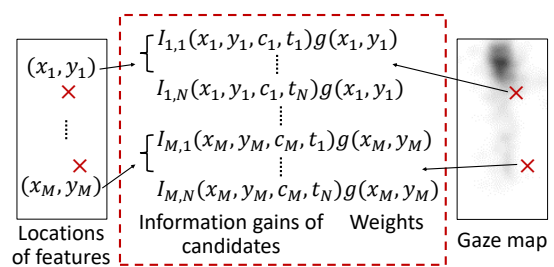

Figure 5: Assigning weights for information gains.

them according to the uniform distribution. In contrast, our method assigns weights for an information gain according to the gaze distribution represented by a gaze map $g(x_i, y_i)$ using the following equation:

$$I'_{i,j}(x_i, y_i, c_i, t_j) = I_{i,j}(x_i, y_i, c_i, t_j)g(x_i, y_i). \qquad (4)$$

We use the parameter set $\{x_i, y_i, c_i, t_j\}$ that corresponds to the maximum information gain $I'_{\max}(x_i, y_i, c_i, t_j)$ as a branch condition from a parent node to a child node. Figure 5 shows an overview of our method. In the figure, a weighted information gain attains a large value when it corresponds to the dark region of the gaze map $g(x_i, y_i)$ where the gaze locations of the observers are gathered.

4 EXPERIMENTS

4.1 Dataset

We evaluated the accuracy of our method on the CUHK dataset included in the PETA dataset (Deng et al., 2014). We used pedestrian images with or without a bias created by a fence in the background surrounding the pedestrians. We included training samples according to the following condition:

- T (Female, Male with a fence),

and test samples according to the following conditions:

- P1 (Female, Male),
- P2 (Female, Male with a fence),
- P3 (Female with a fence, Male),
- P4 (Female with a fence, Male with a fence).

Figure 6 shows examples of the training samples and the test samples. The CUHK dataset consisted of 476 males without a fence, 426 males with a fence, 419 females without a fence, and 355 females with a fence. The size of the pedestrian images was 80×160 pixels.

We used the gaze map shown at the bottom of Figure 2. We generated the gaze map using the procedure described in (Nishiyama et al., 2018). We
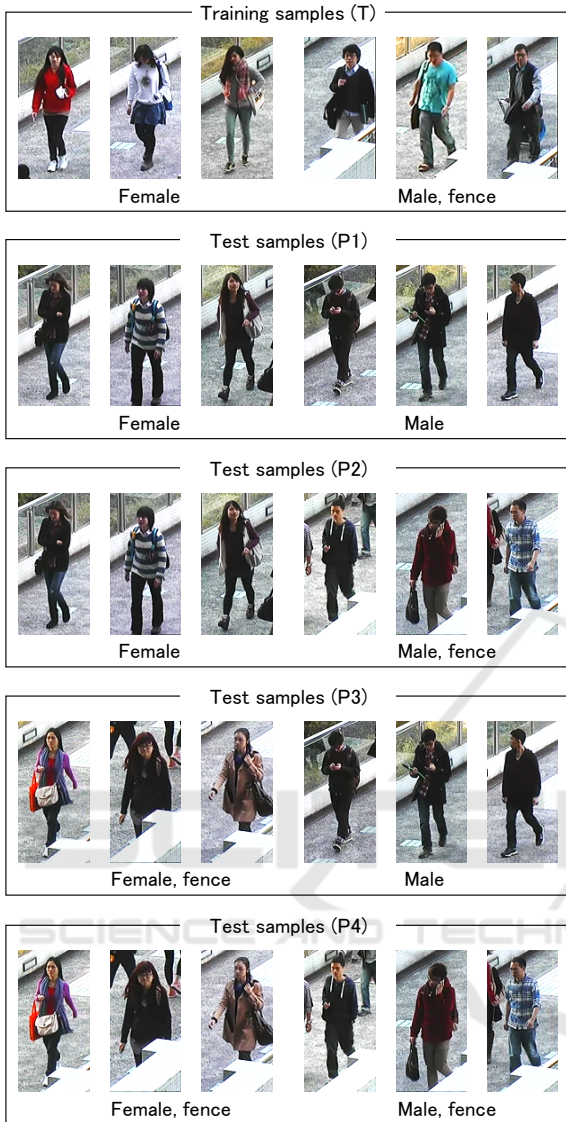
Figure 6: Examples of training samples T and test samples P1 to P4 for gender classification.

used eight stimulus pedestrian images to measure the gaze distribution from 14 observers. The stimulus pedestrian images were randomly selected from the CUHK dataset and were not included in either the training samples or the test samples.

4.2 Basic Gender Classification Performance

We evaluated the gender classification accuracy of the following methods:

- Baseline (Breiman, 2001),
- Random weight (Maudes et al., 2012),

- Our method 1 (Assigning weights for feature selection),
- Our method 2 (Assigning weights for feature values),
- Our method 3 (Assigning weights for information gains).

We generated five test sets by randomly selecting samples from the CUHK dataset. Each training set consisted of 323 males and 323 females, and each test set consisted of 17 males and 17 females. We set the number of random selections for the feature values to $M = 196$, the number of random selections for the thresholds to $N = 50$, the number of decision trees to 200, and the depth of each decision tree to 5.

Figure 7 shows the accuracy of the gender classification for the training sample sets P1 to P4. We see that the accuracies of the baseline and random weight methods were almost the same for (a) to (d). Our methods improve the accuracy for the scenarios where the background differed between the training samples and test samples, for (a), (c), and (d). In particular, assigning weights for the information gain (our method 3) outperformed the other methods for these scenarios. However, our methods degraded the accuracy for (b). To investigate the reason for the degradation, we conducted a comparison using importance maps in the next section.

4.3 Importance Map of the Random Forest

We generated an importance map using the following procedure:

1. We initialized an importance map of the same size as the training samples and set each pixel value to 0.

2. We generated validation samples (out-of-bag) that were not selected as training samples using bootstrap sampling to generate each decision tree.

3. We input the validation samples into each decision tree.

4. We computed an information gain $I_{i,j}(x_i, y_i, c_i, t_j)$ or $I'_{i,j}(x_i, y_i, c_i, t_j)$ for each node that was visited by each validation sample.

5. We added the information gain to the pixel value at position (x_i, y_i) in the importance map. We also added the same value to the eight-neighborhood of (x_i, y_i).

6. We suppressed extremely large values by computing the square root of the added value at each position in the importance map.
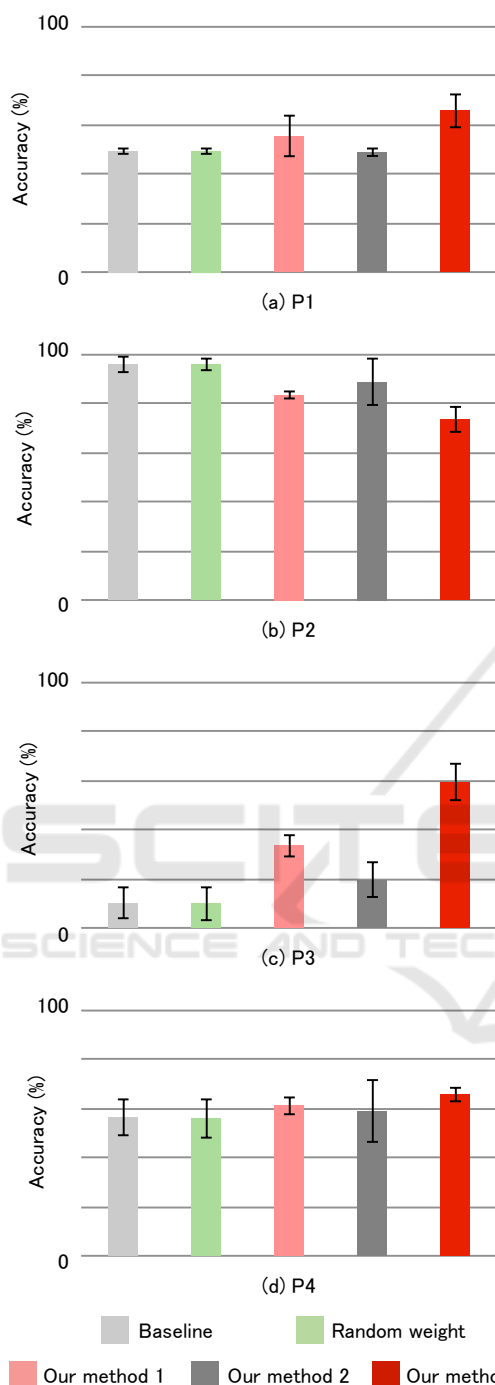
(a) P1

(b) P2

(c) P3

(d) P4

Figure 7: Accuracy of gender classification for training sample sets P1 to P4.

Note that we used the training samples corresponding to condition T described in Section 4.1.

Figure 8 shows the importance maps corresponding to the baseline, random weight, our method 1, our method 2, and our method 3. In the figure, the dark regions represent the areas that each decision
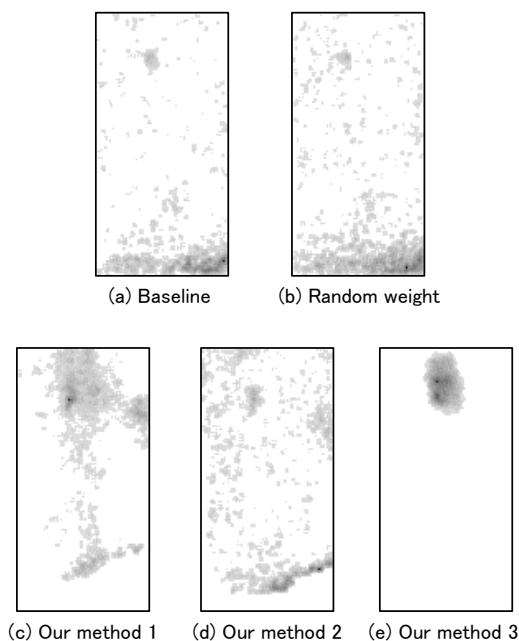

Figure 8: Comparison between the importance maps of the existing methods and our methods.

tree in the random forest regarded as discriminative features when classifying gender. In (a) and (b), we see that the values in the importance map were high where there was a fence in the background. This indicates that the presence or absence of a fence was used for classifying gender by the existing methods. In Figure 8(d), we see that the values of the importance map generated using our method were high for a part of the fence in the background. For this reason, if the weights of the gaze map were even slightly larger than zero, the thresholds for the branch conditions in the decision trees were searched in the small range of the weighted values.

In Figure 8(c) and (e), we see that the values of the importance maps corresponding to our methods were high in the head regions where the observers looked most when judging gender. Note that the values in (c) were also high for the background around the right shoulders. This indicates that the training samples of the CUHK dataset contain a background bias in addition to the fence that we did not originally consider. We confirm that our method avoids the problem of the additional background bias by using the weights according to the gaze distribution.

To investigate the similarity between the importance map and the gaze map, we evaluated the normalized correlation coefficient. We obtained -0.04 for the baseline method, -0.06 for the random weight method, 0.40 for our method 1, -0.02 for our method 2, and 0.76 for our method 3. We confirmed that the

(a) Whole body　(b) Upper body　(c) Head and shoulders

Figure 9: Pedestrian images with manually selected parts.

similarity between the importance map and the gaze map is high when using our method 3 to assign weights for the information gains.

4.4 Comparison using Manually Selected Body Regions

To confirm the effectiveness of using a gaze distribution to generate the random forest, we evaluated the accuracy of our method by comparing it with the existing methods on manually selected body regions. As described in (Li et al., 2013), using manually selected body regions improved the accuracy over the direct use of pedestrian images. We evaluated the methods using the following body regions:

- **Whole Body:** We selected a region containing the whole body by binarizing pixel values of the average pedestrian image from the CUHK dataset. Figure 9(a) shows an example of the whole body region.

- **Upper Body:** We selected a region containing the upper body according to the definitions of the head, shoulders, and torso described in (Wu and Nevatia, 2005). Figure 9(b) shows an example of the upper body region.

- **Head and Shoulders:** We selected a region containing the head and shoulders according to the definition of the head and shoulders described in (Wu and Nevatia, 2005). Figure 9(c) shows an example of the head and shoulders region.

In the figure, the pixel values in the black region are set to zero. We used the same regions for the training samples and the test samples. We generated the random forest using the baseline technique (Breiman, 2001). We used the same experimental conditions as in Section 4.1, with the only difference being the body region selection. For comparison, we use our method 3 (assigning weights for the information gain) that acquired the highest accuracy in Section 4.2.

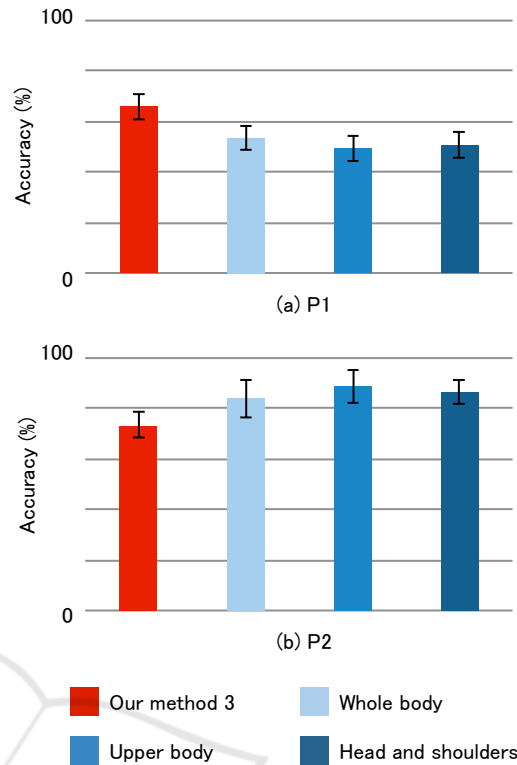Figure 10 shows the accuracies of our method directly on the original images and the existing methods

Figure 10: Accuracy of gender classification when using manually selected image regions.

using manually selected body regions. We see that our method outperformed the existing methods in (a). However, the accuracy of our method was lower than one of the existing methods in (b). To investigate the degradation of the accuracy, we again generated importance maps as described in Section 4.3. Figure 11 shows the importance maps of the existing methods using manually selected body regions. In (a), the existing method using the whole body region emphasized the presence of the fence at the feet of the pedestrians. In (b) and (c), the existing methods using head, shoulder, and torso regions emphasized the background of the right side of the pedestrians in addition to the head regions. The accuracy of our method is superior to that of the existing methods using manually selected body regions because our method correctly ignores the background bias as a feature for gender classification.

5 CONCLUSION

We proposed a gender classification method using gaze distribution to generate a random forest. Our method assigned larger weights for feature selection, feature values, and information gains corresponding

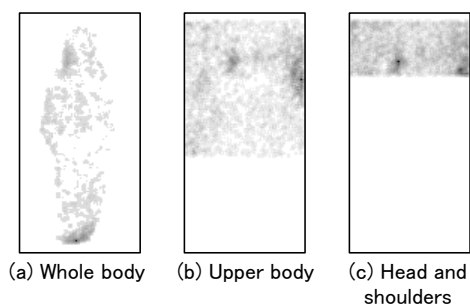(a) Whole body   (b) Upper body   (c) Head and shoulders

Figure 11: Comparison of importance maps when using manually selected body parts.

to the predominant gaze locations of the observers. We confirmed that our method significantly improved the accuracy of gender classification in the presence of a background bias.

In future work, we will further evaluate our method on various datasets using various human attributes. We will also explore the use of the gaze distribution with other machine learning techniques.

ACKNOWLEDGEMENTS

REFERENCES

Amaratunga, D., Cabrera, J., and Lee, Y. S. (2008). Enriched random forests. *Bioinformatics*, 24(18):2010 – 2014.

Antipov, G., Berrani, S., Ruchaud, N., and Dugelay, J. (2015). Learned vs. hand-crafted features for pedestrian gender recognition. In *Proceedings of the 23rd ACM International Conference on Multimedia*, pages 1263–1266.

Breiman, L. (2001). Random forests. *Machine learning*, 45(1):5–32.

Deng, Y., Luo, P., Loy, C., and Tang, X. (2014). Pedestrian attribute recognition at far distance. In *Proceedings of the 22nd ACM International Conference on Multimedia*, pages 789–792.

Gall, J., Yao, A., Razavi, N., Gool, L. V., and Lempitsky, V. (2011). Hough forests for object detection, tracking, and action recognition. *IEEE Transactions on Pattern Analysis and Machine Intelligence*, 33(11):2188–2202.

Li, M., Bao, S., Dong, W., Wang, Y., and Su, Z. (2013). Head-shoulder based gender recognition. In *Proceedings of IEEE International Conference on Image Processing*, pages 2753–2756.

Maudes, J., Rodríguez, J. J., García-Osorio, C., and García-Pedrajas, N. (2012). Random feature weights for decision tree ensemble construction. *Information Fusion*, 13(1):20 – 30.

Murrugarra-Llerena, N. and Kovashka, A. (2017). Learning attributes from human gaze. In *Proceedings of IEEE Winter Conference on Applications of Computer Vision*, pages 510–519.

Nishiyama, M., Matsumoto, R., Yoshimura, H., and Iwai, Y. (2018). Extracting discriminative features using task-oriented gaze maps measured from observers for personal attribute classification. *Pattern Recognition Letters*, 112:241 – 248.

Rokach, L. (2016). Decision forest: Twenty years of research. *Information Fusion*, 27:111 – 125.

Sattar, H., Bulling, A., and Fritz, M. (2017). Predicting the category and attributes of visual search targets using deep gaze pooling. In *Proceedings of IEEE International Conference on Computer Vision Workshops*, pages 2740–2748.

Schumann, A. and Stiefelhagen, R. (2017). Person re-identification by deep learning attribute-complementary information. In *Proceedings of the IEEE Conference on Computer Vision and Pattern Recognition Workshops*, pages 1435–1443.

Winham, S. J., Freimuth, R. R., and Biernacka, J. M. (2013). A weighted random forests approach to improve predictive performance. *Statistical Analysis and Data Mining*, 6(6):496–505.

Wu, B. and Nevatia, R. (2005). Detection of multiple, partially occluded humans in a single image by bayesian combination of edgelet part detectors. In *Proceedings of Tenth IEEE International Conference on Computer Vision*, volume 1, pages 90–97.